Available online at www.sciencedirect.com
ScienceDirect
Trans. Nonferrous Met. Soc. China 22(2012) 2498−2503
Transactions of Nonferrous Metals Society of China
www.tnmsc.cn

Interface characteristics of Al_2O_3−13%TiO_2 ceramic coatings prepared by laser cladding

GAO Xue-song[1, 2], TIAN Zong-jun[2], LIU Zhi-dong[2], SHEN Li-da[2]

1. School of Mechanical Engineering, Southeast University, Nanjing 210018, China;
2. College of Mechanical and Electrical Engineering,
Nanjing University of Aeronautics and Astronautics, Nanjing 210016, China

Received 9 July 2012; accepted 17 August 2012

Abstract: Al_2O_3−13%TiO_2 (mass fraction) coatings, prepared by laser cladding on nickel-based alloy, were heated using high frequency induction sources. The coating microstructure and the interface between bond coating and ceramic coating were characterized by SEM, XRD and EDS. The results show that two-layer substructure exists in the ceramic coating: one layer evolving from fully melted region where the sintered grains grow fully; another layer resembling the liquid-phase-sintered structure consisting of three-dimensional net where the melted Al_2O_3 particles are embedded in the TiO_2-rich matrix. The mechanism of the two-layer substructure formation is also explained in terms of the melting and flattening behavior of the powders during laser cladding processing. The spinel compounds $NiAl_2O_4$ and acicular compounds Cr_2O_3 are discovered in the interface between bond coating and ceramic coating. It proves that the chemical reactions in the laser cladding process will significantly enhance the coating adhesion.
Key words: ceramic coating; nickel alloy; laser cladding; Al_2O_3−TiO_2; high frequency induction

1 Introduction

Ceramics are widely applied for protective coating because of their excellent wear, corrosion, heat and high temperature oxidation resistance [1−3]. However, ceramic coatings show low adhesion prepared by surface coating technique due to huge difference between ceramic material and metal matrix material in physical performance. Ceramic coatings commonly tend to fail as a result of huge thermal stress at high temperature environment [4−6].

Laser cladding technology has been proven a promising method for ceramic coating preparation, due to its low power consumption, short time, high efficiency, high relative density and fine grain size [7,8]. The grain size is one of the important factors which influence the performance of ceramic coatings [9,10]; therefore, the laser cladding technology is also extensively considered a potential method that control grain growth. However, ceramic and metals are difficult to combine because of their different physical properties under the act of laser heat source [11,12]. For above reasons, the laser cladding technology was only used to remelt ceramic coating prepared by plasma-sprayed, as an effort to eliminate hole and typical lamellar stacking defects [13, 14]. Up to now, few investigations were done on laser cladding ceramic coatings.

In the present study, Al_2O_3−13%TiO_2 (mass fraction) ceramic coatings were prepared by laser cladding. The effect of laser cladding on microstructure of the ceramic the coatings was studied.

2 Experimental

2.1 Materials

GH4169 nickel-based alloy was chosen as the substrate material due to frequently working at high temperature and on corrosion [15]. The chemical composition (mass fraction, %) of the substrate material is listed as follows: Ni 53.00; Cr 20.00; Nb 5.10; Mo 3.00; Ti 1.00; Co 0.70; Al 0.5; Si 0.32; Mn 0.30; Cu 0.28; C 0.07; Ca 0.01; P 0.01; S 0.01; B 0.01; Mg 0.01; and the remainder Fe. The specimens with coupons in size of 40 mm×40 mm×5 mm were cut by wire electrical discharge machining (WEDM). To reduce thermal–physical

Foundation item: Project (59975046) supported by the National Natural Science Foundation of China
Corresponding author: GAO Xue-song; Tel: +86-13770649527; E-mail: gaoxuesong_2001@163.com
DOI: 10.1016/S1003-6326(11)61491-X

property difference between ceramic coating and GH4169 alloy, superalloy powders (sized 44–104 μm), as a function of bond coating, was used with rare earth oxides addition (provided by Institute of Metal Materials, Beijing General Research Institute of Mining and Metallurgy, China), and the nominal chemical composition was Ni−20Co−18Cr−15Al−2Y_2O_3 (mass fraction, %).

In the present study, the nano agglomerated powders were used, which were marked by Nanox S2613P (Inframat Corporation, USA), and the nominal chemical composition was Al_2O_3−13%TiO_2. The powders were agglomerated and sintered with mixture of nanosized alumina and titania particles. The sizes of the powders varied from 10 μm to 50 μm (Fig. 1(a)). The high magnification image of cross-section (see Fig. 1(b)) exhibits a porous microstructure and the grain size of the nanoparticles ranges from 0.05 μm to 0.2 μm. The ceramic powders were preplaced on the plate with an organic binder. The thickness of the coating was about 0.5 mm.

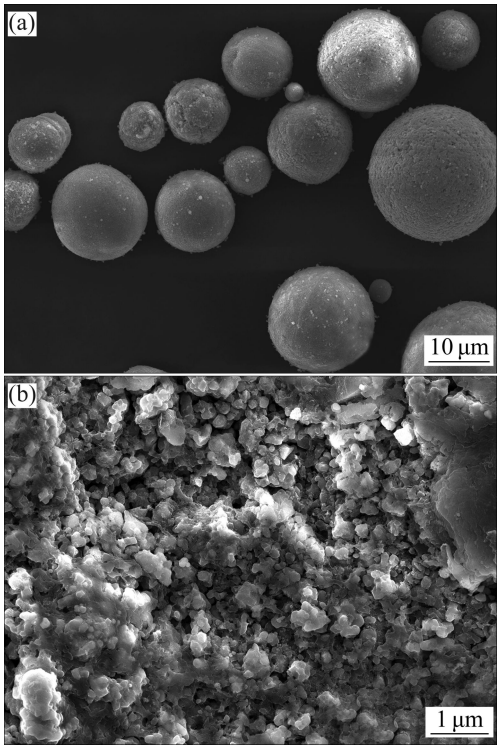

Fig. 1 SEM images of as-prepared Al_2O_3−13%TiO_2 powders: (a) Surface morphology; (b) Cross-sectional structure

2.2 Preparation of Al_2O_3−13%TiO_2 coating

Laser surface cladding experiments were performed on a 2 kW CO_2 laser (SLCF−12 25, China). During laser cladding, high frequency induction heating equipment was used to slow cooling. The laser cladding parameters, optimized from a required number of preliminary experiments, were laser beam moving velocity of 1200 mm/min and laser output power of 900 W. The laser beam was defocused to a spot of 3 mm in diameter on the surface of the coating; argon gas was blown into the molten pool to provide shielding during laser cladding. Assisted heating was performed by a high frequency induction heating equipment (HFP−30, China), with 100 kHz oscillation frequency, ensuring a working surface over 1000 °C. Figure 2 shows the Al_2O_3−13%TiO_2 ceramic specimen prepared by laser cladding.

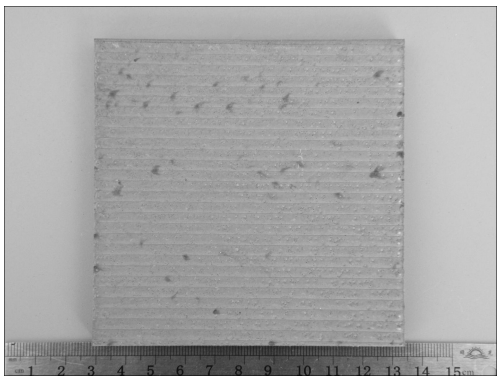

Fig. 2 Al_2O_3−13%TiO_2 ceramic specimen prepared by laser cladding

2.3 Characterization of coating

A JSM7100Ffield emission scanning electron microscopy (JEOL, Japan) integrated with an X-ray energy-dispersive spectroscopy (EDS) was employed to investigate the microstructure of agglomerated powders and the coating. The phase compositions of the coatings were examined by an X-ray diffractometer (XRD) (D/max2400, Rigaku, Japan).

3 Results and discussion

3.1 Microstructure of the coating

SEM observations show that the coatings have a smooth surface and are free of porosities and cracks (Fig. 3(a)). In Fig. 3(a), there are nickel alloy substrate, MCrAlY bond coating and Al_2O_3−13%TiO_2 ceramic coating from left to right. The thickness of the bond coating after laser processing is about 147 μm and the thickness of ceramic coating after laser processing is about 140 μm.

Figure 3(b) presents a high magnification cross-sectional microstructure of ceramic coating, bond coating and substrate. The excellent mechanical bonding interface is formed between the ceramic coating and bond coating, as well as that between the bond coating and substrate. Laser cladding ceramic coating reveals two kinds of structural features, fully melted region and liquid-phase sintered region. Figure 3(c) shows the high magnification cross-sectional image of ceramic coatings and bond layer. It can be seen that the ceramic coating

and bonding coating are combined tightly. Meanwhile, there are short-range spread features between them. It is proved that the wettability of ceramic coating and bond coating is improved significantly by the compound effects from high-frequency induction and laser.

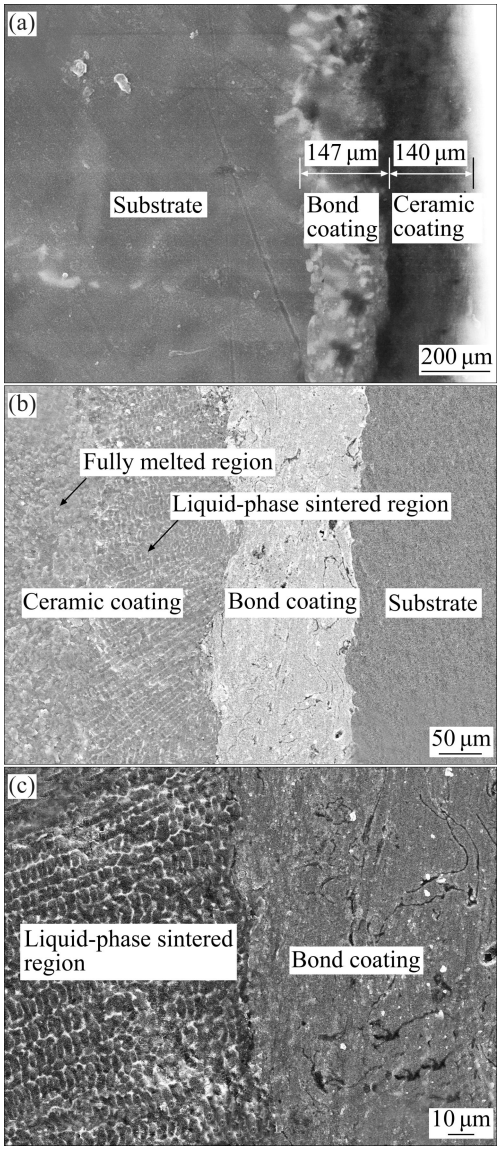

Fig. 3 Cross-sectional SEM morphologies of laser cladding coating: (a) Overview; (b) High magnification of ceramic coating, bond coating and substrate; (c) High magnification of bond coating and ceramic coating

SEM morphologies of the ceramic coating are shown in Fig. 4. Two kinds of microstructures can be seen in the ceramic coating at micro-scaled view. In the fully melted region (Fig. 4(a)), a typical laser sintering structure appears as the conventional coating has fine equiaxed grains. Liquid-phase sintered region (Fig. 4(b)) exhibits a large-area three-dimensional net or skeleton-like structure as proved in the Refs. [3,13,16,17]. Although the structure is found in the coating prepared by plasma sprayed, there are only local areas compared with the coating prepared by laser cladding. The structure is composed of submicron grains and thin net walls which surround the grains. The submicron particles are embedded in the thin-net-walls structure matrix. Figure 5 shows the EDS analysis of net structures in liquid-phase sintered. The EDS analysis results exhibit that the submicron grains in the net structures are Al_2O_3-rich particles, and the thin net walls belong to TiO_2-rich matrix microstructure.

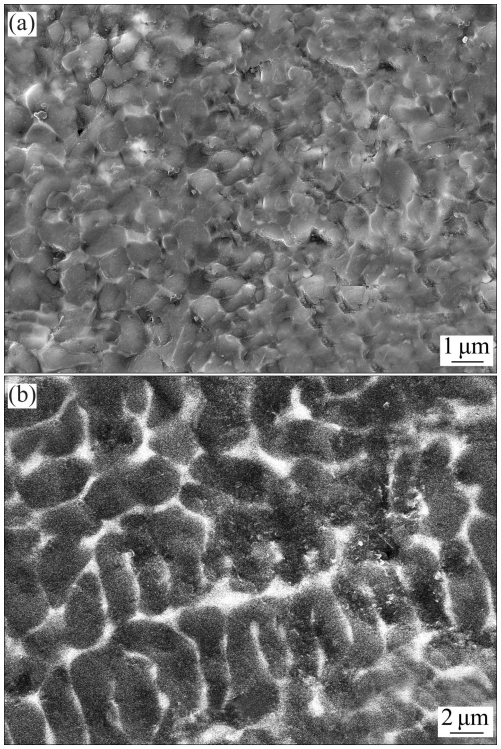

Fig. 4 High magnification SEM images of ceramic coating: (a) Fully melted region; (b) Liquid-phase sintered region

The microstructural formation of ceramic coating can be better understood with the help of a model indicating the microstructural evolution at every stage following the processing procedures of reconstitution, as shown in Fig. 6. When the agglomerated Al_2O_3−13%TiO_2 powders are employed for laser cladding, the temperature rapidly increases during laser irradiating the surface of ceramic coating. It could be assumed that the superficial temperature of the power is obviously beyond 2045 °C (melting point of Al_2O_3) [18], agglomerated powders will be completely melted, then a fully melted region as shown in Fig. 6(a) is formed. The temperature decreases with the distance increasing to surface due to the conductivity, when the temperature decreases below 2045 °C, meanwhile beyond 1840 °C [18] (melting point of TiO_2), the region will be liquid-phase sintered because the temperature of this region is between 1840 °C and 2045 °C. Consequently, TiO_2 is melted but Al_2O_3 is still

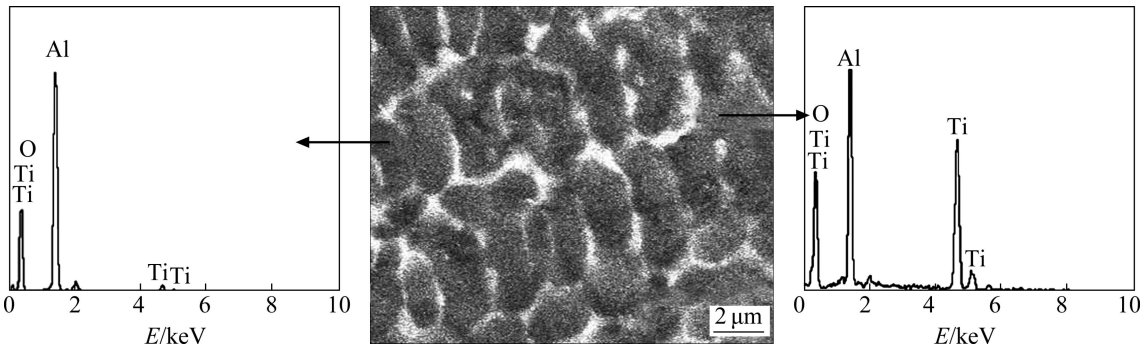

Fig. 5 EDS patterns of liquid-phase sintered region

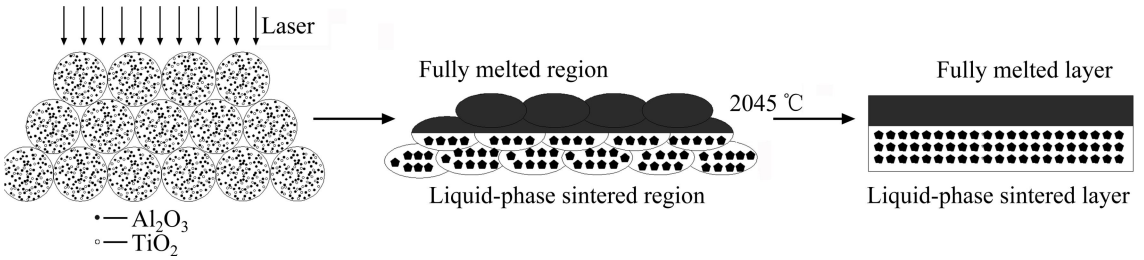

Fig. 6 Schematic illustration of microstructural evolution model indicating evolution of ceramic coating: (a) Early stage; (b) Middle stage; (c) Later stage

solid, the melted TiO_2 transforms to the liquid phase and fills in the gaps among Al_2O_3 solid phases. The microstructural characteristics of the liquid-phase sintered region (Fig. 4(b)) result from the selective melting of TiO_2 during laser cladding.

3.2 Interaction products of ceramic coating/ NiCoCrAl−Y_2O_3 bond coating

The bonding coating and substrate are deeply-eroded in order to observe the reaction microstructure and XRD patterns of the interface (Figs. 7(a) and (b)). The interface between the bond coating and ceramic coating is unevenness, and the compounds produce on the interface. The XRD patterns of interface show that the main phases are Al_2O_3, $NiAl_2O_4$, Cr_2O_3 and $Al_2Ti_7O_{15}$. By comparing with the composition of Al_2O_3−13%TiO_2 powders, $NiAl_2O_4$ and Cr_2O_3 are new phases produced on the interface. It shows that there are chemical reactions on the interface, which significantly increase the binding force of ceramic coating [19].

Figures 7(c)–(f) show the interaction products on the interface between the ceramic coating and the bond coating. It can be seen that many spinel compounds produced on the reaction interface (Figs. 7(c) and (d)), and the grain size of spinel compounds is about 1 μm. According to the EDS and XRD (Fig. 7(b)) results, the spinel compounds are $NiAl_2O_4$. Meanwhile, the acicular compounds are found on the interface (Fig. 7(c)), and the length of acicular compounds is in the range from 5 μm to 8 μm. According to the EDS and XRD (Fig. 7(b)) results, the acicular compounds are Cr_2O_3.

Although many studies were carried out on the ceramic coatings prepared by laser cladding, most of the interfaces belong to the mechanical bonding due to their different physical properties and instantaneous high temperature effect of laser [11,13,20]. This work applied high frequency induction assisted laser cladding in order to obtain enough reaction time, and the interactive short-range diffusion will occur between coatings. Finally, the interaction products of ceramic coating/ NiCoCrAl−Y_2O_3 bond coating will be formed.

As an adhesive layer material, NiCoCrAl−Y_2O_3 has small differences in physical properties from ceramic materials. Elements such as Cr and Ni in the adhesive layer material are easy to be oxidized and the Gibbs free energies to generate Cr_2O_3 and NiO are −548 kJ/mol and −265 kJ/mol, respectively. As the formation free energy is relatively low, the following reactions will occur in the first place:

$$Cr+O\longrightarrow Cr_2O_3 \quad (1)$$

$$Ni+O\longrightarrow NiO \quad (2)$$

NiO and Cr_2O_3 have a strong affinity. At a certain temperature, NiO and Cr_2O_3 overcome the activation energy and carry out the interfacial reaction [21,22]:

$$Ni+Al_2O_3\longrightarrow NiAl_2O_4 \quad (3)$$

In conclusion, the high frequency induction assisted laser cladding process includes the following steps: 1) In the rapid heating effect of laser, the elements Ni and Cr

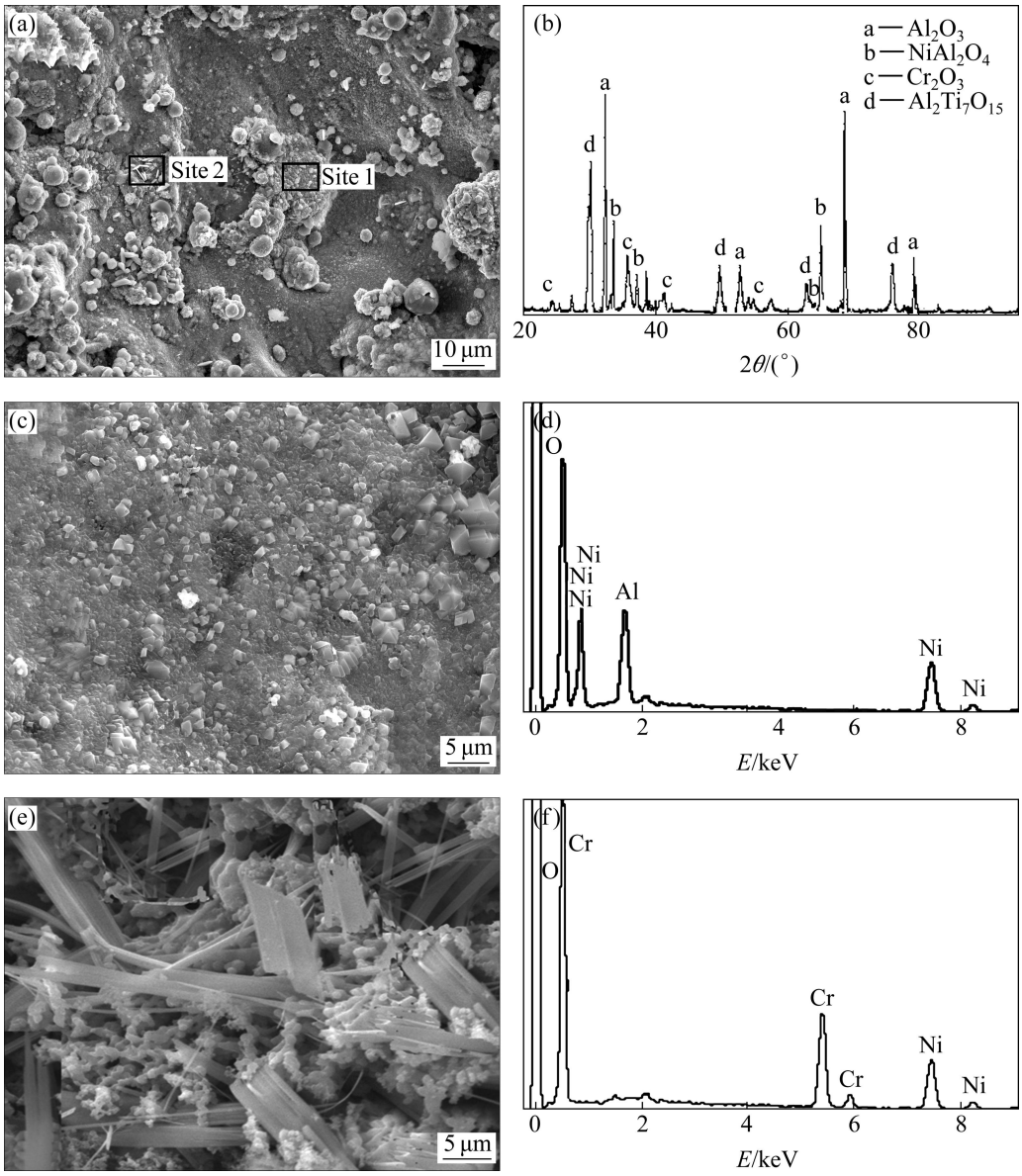

Fig. 7 SEM morphologies of interface between bond coating and ceramic coating: (a) Overview; (b) XRD pattern; (c) Higher magnification view of site 1; (d) EDS pattern of site 1; (e) Higher magnification view of site 2; (f) EDS pattern of site 2

in adhesive layer quickly diffuse into ceramic layer; 2) Ni and Cr in the diffusion process will undergo the oxidation reactions and generate NiO and Cr_2O_3; 3) Generated NiO will react with Al_2O_3 in ceramic layer, and form $NiAl_2O_4$, thereby the binding properties of the coating are enhanced.

4 Conclusions

1) The laser cladding Al_2O_3−13%TiO_2 coating shows a two-layer substructure composed of fully melted layer and liquid-phase sintered layer. The liquid-phase sintered layer exhibits a three-dimensional net: Al_2O_3 particles embedded in the TiO_2-rich matrix.

2) The fully melted layer and liquid-phase sintered layer of the coating derive from temperature changes. On the surface of the ceramic coating, the temperature is obviously beyond 2045 °C (melting point of Al_2O_3), the agglomerated powders are completely melted, then a fully melted layer is formed. The temperature decreases with the distance increasing to surface due to conductivity. When the temperature decreases below 2045 °C, meanwhile beyond 1840 °C (melting point of TiO_2), the liquid-phase sintered layer is formed.

3) The spinel compound $NiAl_2O_4$ and acicular compound Cr_2O_3 are discovered on the interface between the bond coating and ceramic coating. The result proves that chemical reaction occurs on the interface, and the interactive short-range diffusion between coatings occurs, thereby the effective interfacial bonding is formed.

References

[1] EVANS H E. Oxidation failure of TBC systems: An assessment of mechanisms [J]. Surface & Coatings Technology, 2011, 206(7): 1512−1521.

[2] GUO Q Q, JIANG B L, LI J P. Corrosion resistance of micro-arc oxidized ceramic coating on cast hypereutectic alloy [J]. Transactions of Nonferrous Metals Society of China, 2010, 20(11): 2204−2207.

[3] WANG D S, TIAN Z J, SHEN L D, LIU Z D, HUA Y H. Influences of laser remelting on microstructure of nanostructured Al_2O_3–13 wt.%TiO_2 coatings fabricated by plasma spraying [J]. Applied Surface Science, 2009, 255: 4606−4610.

[4] BHATNAGAR H, GHOSH S, WALTER M E. A parametric study of damage initiation and propagation in EB-PVD thermal barrier coatings [J]. Mechanics of Materials, 2010, 42(1): 96−107.

[5] HAN J C. Thermal shock resistance of ceramic coatings [J]. Acta Materialia, 2007, 55(10): 3573−3581

[6] WANG Y L, JIANG Z H, YAO Z P. Microstructure, bonding strength and thermal shock resistance of ceramic coatings on steels prepared by plasma electrolytic oxidation [J]. Applied Surface Science, 2009, 256(3): 650−656.

[7] ZHU C, LI P, JAVED A. An investigation on the microstructure and oxidation behavior of laser remelted air plasma sprayed thermal barrier coatings [J]. Surface & Coatings Technology, 206(18): 3739−3746.

[8] BAI PK, CHENG J, LIU B. Selective laser sintering of polymer-coated Al_2O_3/ZrO_2/TiC ceramic powder [J]. Transactions of Nonferrous Metals Society of China, 2005, 15(2): 261−265.

[9] MURTY S V S, TORIZUKA S, NAGAI K, KITAI T, KOGO Y. Effect of initial grain size on evolved ferrite grain size during high Z large strain deformation [J]. Materials Science Technology, 2010, 26(7): 879−885.

[10] TSAO L C, CHANG S Y, LEE C I, SUN W H, HUANG C H. Effects of nano-Al_2O_3 additions on microstructure development and hardness of Sn3.5Ag0.5Cu solder [J]. Materials & Design, 2010, 31(10): 4831−4835.

[11] BERTRAND P, BAYLE F, COMBE C. Ceramic components manufacturing by selective laser sintering [J]. Applied Surface Science, 2007, 254(4): 989−992

[12] SUN C N, BALDRIDGE T, GUPTA M C. Fabrication of ZrB_2−Zr cermet using laser sintering technique [J]. Materials Letters, 2009, 63(28): 2529−2531.

[13] WANG Y, LI C G, GUO L X, TIAN W. Laser remelting of plasma sprayed nanostructured Al_2O_3−TiO_2 coatings at different laser power [J]. Surface & Coatings Technology, 2010, 204(21−22): 3559−3566

[14] SONG E P, AHN J, LEE S, KIM N J. Microstructure and wear resistance of nanostructured Al_2O_3−8wt.%TiO_2 coatings plasma-sprayed with nanopowders [J]. Surface & Coatings Technology, 2006, 201: 1309−1315.

[15] LIU Y, WANG L, HE S S, FENG F, LU X D, ZHANG B J. Effect of long-term aging on dynamic tensile deformation behavior of GH4169 alloy [J]. Acta Metallurgica Sinica, 2012, 48(1): 49−55. (in Chinese)

[16] WANG D S, TIAN Z J, SHEN L D, LIU Z D, HUANG Y H. Microstructural characteristics and formation mechanism of Al_2O_3–13wt.% TiO_2 coatings plasma-sprayed with nanostructured agglomerated powders [J]. Surface & Coatings Technology, 2009, 203: 1298−1303.

[17] LUO H, GOBERMAN D, SHAW L. Indentation fracture behavior of plasma-sprayed nanostructured Al_2O_3–13wt.%TiO_2 coatings [J]. Materials Science and Engineering A, 2003, 346: 237−245.

[18] GOBERMAN D, SOHN Y H, SHAW L, JORDAN E, GELL M. Microstructure development of Al_2O_3–13wt.%TiO_2 plasma sprayed coatings derived from nanocrystalline powders [J]. Acta Materialia, 2002, 50: 1141−1152

[19] DING W F, XU A H, CHEN Z Z, CHENG ZE, FU Y C. A study on effect of TiB_2 contents on reactive products and compressive strength of brazed CBN grains [J]. Surface and Interface Analysis, 2009, 41(3): 238−243.

[20] GAO X S, TIAN Z J, HUANG Y H, LIU Z D, SHEN L D. Al_2O_3−TiO_2 ceramic coating prepared by laser cladding[J]. Journal of Jiangsu University, 2011, 32(6):720−723. (in Chinese)

[21] JACKSON R D, TAYLOR M P, EVANS H E. Oxidation study of an EB-PVD MCrAlY thermal barrier coating systems [J]. Oxidation of Metals, 2011, 76(3−4): 259−271.

[22] SLOOF W G, NIJDAM T J. On the high-temperature oxidation of MCrAlY coatings [J]. International Journal of Materials Research, 2009, 100(10): 1318−1330.

激光熔覆 Al_2O_3–13%TiO_2 陶瓷涂层的界面特征

高雪松[1,2]，田宗军[2]，刘志东[2]，沈理达[2]

1. 东南大学 机械工程学院，南京 210018；2. 南京航空航天大学 机电学院，南京 210016

摘 要：利用高频辅助激光熔覆技术在镍基合金上制备 Al_2O_3−13%TiO_2(质量分数)陶瓷涂层。采用 SEM、XRD 和 EDS 等方法分析陶瓷涂层的微观结构和陶瓷层与粘结层之间的结合界面。结果表明：陶瓷层出现了完全熔化区和液相烧结区双层结构，其中，完全熔化区颗粒充分烧结长大，而液相烧结区则出现了三维网状结构，该三维网状结构由熔化的 TiO_2 相包裹 Al_2O_3 颗粒形成。通过激光熔覆作用下的粉末熔化和扁平化行为解释双层结构形成机理。同时，在陶瓷层与粘结层的结合界面上发现具有尖晶石结构的 $NiAl_2O_4$ 和针状结构的 Cr_2O_3，证明在激光熔覆过程中发生的化学反应可以有效增加陶瓷层与粘结层的结合强度。

关键词：陶瓷涂层；镍基合金；激光熔覆；Al_2O_3−TiO_2；高频辅助

(Edited by HE Xue-feng)